



Laser texturing of glass for modified surface energy and hydrophobicity

Abdul Fattah Mohamad Tahir ^{1,2}, Syarifah Nur Aqida Syed Ahmad ^{3,4*}, Izwan Ismail ¹, Nur Ezrin Mad Sariff ⁵

¹ Faculty of Manufacturing and Mechatronics Engineering Technology, Universiti Malaysia Pahang Al-Sultan Abdullah, MALAYSIA.

² Department of Automotive Manufacturing, Kolej Kemahiran Tinggi MARA Kuantan, MALAYSIA.

³ Faculty of Mechanical and Automotive Engineering Technology, Universiti Malaysia Pahang Al-Sultan Abdullah, MALAYSIA.

⁴ Universiti Malaysia Pahang Al-Sultan Abdullah, Automotive Engineering Centre, MALAYSIA.

⁵ Department of Manufacturing Design, Kolej Kemahiran Tinggi MARA Kuantan, MALAYSIA.

*Corresponding author: aqida@umpsa.edu.my

KEYWORDS	ABSTRACT
Maximum profile peak height Hydrophobic Laser surface modification Fiber laser Surface Energy	The use of hazardous chemicals as a secondary process in glass surface modification contradicts the aspirations of Sustainable Development Goals. Opting for laser surface texturing, hydrophilic soda lime silica glass surface can be transformed into a hydrophobic state by manipulating its surface energy. To date, findings on the effect of roughness profile on surface energy are still limited. This study investigated a facile methodology for examining wettability, surface energy and surface topography resulting from variations in laser fluence, hatch pattern and spacing. The assessment of wettability according to ASTM D7490 and ASTM D7334 was conducted using distilled water, while surface topography was evaluated based on the ISO4287 standard. The sessile drop test reveals that samples with a spacing interval of 0.06 mm recorded a maximum water contact angle of 96° which equivalent to 26.98 mJ/m ² ; resulted in complete transformation into a hydrophobic state. Samples with Rz value greater than 23 μm generally exhibited lower wettability surface compared to pristine glass and promoted lower surface energy. These findings are significant for tailoring the roughness profile of glass using laser processing technique, which has the potential to modify the wettability of glass.

Received 17 July 2024; received in revised form 2 November 2024; accepted 20 January 2025.

To cite this article: Mohamad Tahir et al., (2025). Laser texturing of glass for modified surface energy and hydrophobicity. *Jurnal Tribologi* 44, pp.16-40.

1.0 INTRODUCTION

Surface modification of glass through laser processing has created a new branch of emerging research, as this process has shown promising outcomes, especially in terms of surface wettability. Non-contact application, fast processing with low-cost operation in a standard working environment without concerns for fumes and hazardous gases have demonstrated the advantages of this method. The combination of galvanometric features with fast processing speed enables high precision in the fabrication of fine complex patterns on the material surface. Current surface processing methods such as mechanical polishing, grinding, etching and sandblasting have proven to have limitations (Comesaña et al., 2019).

Laser texturing has been used widely in the surface structuring field to alter the material wettability. Numerous studies have focused on metallic materials, exploring how to modify the surface wettability to achieve either superhydrophilic or superhydrophobic states (Liu et al., 2024; W. Qian et al., 2020; Y. Qian et al., 2023; Yamaguchi & Kato, 2023; Yusuf et al., 2022). Recently, the motivation to modify glass wettability has gained significant interest rapidly as new emerging technologies evolved. The use of nanosecond laser at an ultraviolet wavelength to produce micro and nano-scale structures has proven to change the wettability of glass (Dinh et al., 2020; Jing et al., 2022; Najwa et al., 2024; Nategh et al., 2021; Nguyen et al., 2021)

Despite the development of established methods, the multiple-step processes that require hazardous chemicals as a secondary treatment have proven to be a drawback in the implementation of these methods (Dinh et al., 2020; Dinh et al., 2020; Soldera et al., 2021). Wettability reduction can be achieved in several ways, including the development of low surface energy on the working material's surface. Materials with low surface energy enable water droplets to retain their surface tension and their spherical shape (Goswami et al., 2021). This objective can be achieved by modifying the chemical composition, reducing the surface energy and generating microstructures through roughness modification. A review by Jothi Prakash & Prasanth (2021) indicated that surface roughness has been one of the profound effects in modifying the wettability of a solid surface. Rough topographies related to surface roughness directly affect the surface energy and surface chemistry, influencing the water droplet formation and leading to changes in the contact angle.

In terms of surface chemistry, the reduction of polar energy can transform hydrophilic surfaces into hydrophobic ones (Ahmad et al., 2018). The usage of fluorine-based chemicals as low surface energy agents to induce hydrophobicity was implemented by various researchers (Jing et al., 2022; Lin et al., 2018; Ouchene et al., 2023; B. Wang et al., 2017; Yang et al., 2020; J. Zhang et al., 2020). However, these low surface energy agents, which act as catalysts can contribute to environmental pollution.

This study aims to investigate a toxic-free process, a single-step method of modifying commercial soda lime silica glass through laser texturing. The process evaluates the effect of hatch spacing, laser fluence and hatch patterns on surface wettability, topography, surface energy and surface chemistry in accordance with established standards. This cost-effective process presents interesting possibilities in determining the wetting regime of textured soda lime silica glass, thus adapting these recyclable materials into a bigger scope of functional applications.

2.0 METHODOLOGY

2.1 Sample Preparation

Soda-lime glass with a thickness of 1 mm was used as the sample material for this research. The glass pieces, measuring 76x25 mm², are hydrophilic soda lime glass that contains the composition listed in Table 1. Before the laser texturing process, the samples were cleaned intensively (Figure 1) to prevent contamination on the working surface.

Table 1: Composition of pristine soda lime glass.

Composition	SiO ₂	Na ₂ O	K ₂ O	CaO	MgO	Al ₂ O ₃	Fe ₂ O ₃
Wt%	72.00	14.50	0.3	7.05	3.95	1.65	0.06

The cleaning process involved washing the samples with 99.9% ethanol for 5 minutes, followed by a rinse with Isopropyl Alcohol (IPA) and Distilled Water (DW) for another 5 minutes with each solution (Bakhtiari et al., 2022; X. Li et al., 2023; Lin et al., 2018; Luo et al., 2023). Subsequently, the samples were black-coated to form a thin opaque layer that enhanced laser absorption. The samples were left dried at room temperature for 24 hours. Since this research work used a Near-Infrared Laser, laser absorption on transparent materials was a key challenge in implementing Direct Laser Texturing (DLT), and the opaque coating served as an effective solution for the surface modification process (Gao et al., 2022; Mulko et al., 2022; Qahtan et al., 2017; Z. Wang et al., 2023).

2.2 Laser Processing

A Near-Infrared Laser operated at 1065 nm wavelength with a maximum pulsed energy of 2 mJ was utilized in this research. The fiber laser system is a 50-watt laser machine (CK-FB3D50, IDI™, Singapore) that capable of texturing up to 1000x1000 mm² area with a scanning speed of up to 7000 mm/s using galvo application. Two types of hatch patterns illustrated in Figure 2 with variations hatch spacing and laser fluence were employed in this experimental work after conducting a series of preliminary trials. Fixed laser parameters included an average power of 50 watts, a power density of 84 kW/mm², a duty cycle of 30%, a laser beam diameter of 50 μm and beam overlapping of 99%. Throughout the experiment, the laser beam was focused on the top surface of the coated samples with a processing speed of 20 mm/s. Meanwhile, two levels of laser fluence were varied resulted from the pulse duration of 5 μsec (60 kHz; 212.2 mJ/mm²) and 3 μsec (120 kHz; 424.4 mJ/mm²). Figure 2 illustrates the schematic figure of how the experiment was executed using a fiber laser machine.

Using a Full Factorial method, a total of eight experimental runs were performed with variations parameters (in Table 2) to evaluate the effect of each laser parameter on surface wettability, surface energy and surface topography. After the laser texturing process, the modified samples were cleaned using IPA and distilled water using an ultrasonic bath for 5 minutes each.

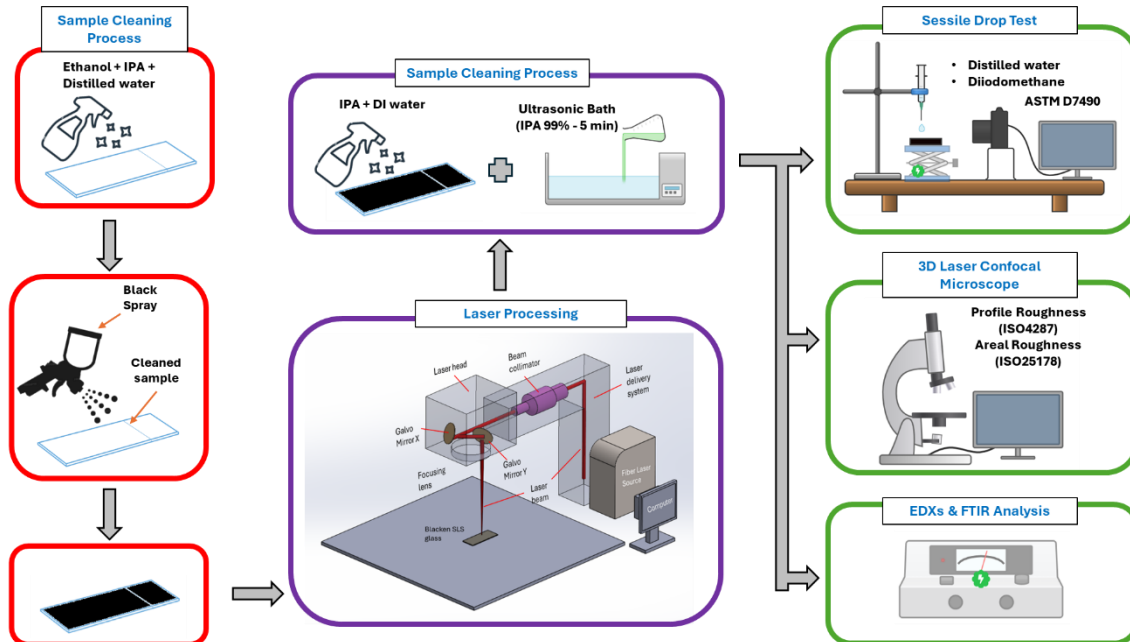


Figure 1: Experimental methodology for laser texturing of glass.

Table 2 : Laser texturing parameters.

Laser Parameters	Code	Units	Low	High
Hatch spacing	A	μm	60	500
Laser fluence	B	mJ/mm^2	212.2	424.4
Hatch pattern	C		Line Hatch	Cross Hatch

2.3 Characterization

2.3.1 Contact Angle Measurement

Surface wettability was measured using the sessile drop test setup, which include a gas-tight threaded plunger syringe (1001 Luer Tip, Hamilton™, USA) equipped with a hypodermic needle. A 6 μL droplet of distilled water was used as measuring liquid at room temperature in accordance with ASTM D7334 standard. Three droplets were carefully placed at different locations and six measurements were made using ImageJ™ software with the Drop Shape Analysis plugin (Stalder et al., 2006), calibrated using the droplet diameter method (Gunerhan & Genc Oztoprak, 2023). Measurements were taken after 5 seconds to stabilize the modified samples. An average value was calculated and determined as the final contact angle.

2.3.2 Surface Energy Evaluation

Surface energy (γ_s) was measured by comparing the contact angles of distilled water (θ_w) and Diiodomethane (θ_i). These two values were then substituted in two separate simplified equations (Eq. 1 and Eq. 2) of the Owens-Wendt-Keable (OWK) to calculate the dispersion (γ^d) and polar components (γ^p) of surface energy. The total surface energy of the glass was determined as the

sum of the polar (γ^p) and dispersion (γ^d). Surface energy calculations on the procedure are based on the ASTM D7490 standard with the value for its components of these liquids' energy as tabulated in Table 3.

Table 3: Polar and dispersion components for distilled water and Diiodomethane.

Measuring liquids	Surface components (mJ/m ²)		
	γ_L	γ_L^d	γ_L^p
Distilled water (w)	72.8	21.8	51.0
Diiodomethane (i)	50.8	49.5	1.3

$$72.8(1 + \cos \theta_w)/2 = \left[(21.8\gamma_s^d)^{1/2} + (51.0\gamma_s^p)^{1/2} \right] \quad \text{Eq. 1}$$

$$50.8(1 + \cos \theta_i)/2 = \left[(49.5\gamma_s^d)^{1/2} + (1.3\gamma_s^p)^{1/2} \right] \quad \text{Eq. 2}$$

2.3.3 Surface Roughness

Surface roughness was evaluated using a 3D Laser Confocal Microscope (OLS5000, Olympus LEXT™, Japan) following ISO4287 standards. An area of 646x646 μm^2 was inspected to measure profile roughness (Rp, Rv, Rz, and Ra).

2.3.4 Surface Morphology Examination

Surface morphologies were characterized using Scanning Electron Microscope (JSM-IT200, JOEL™, Japan) with magnification setup of 500 μm (35 \times) and 5 μm (5000 \times). Further investigation was carried out using Energy Dispersive X-ray (JSM-IT200, JOEL™, Japan) to evaluate the changes in chemical composition. Final examinations on the surface analysis were done using Attenuated Total Reflection Infrared Spectroscopy (Nicolet iS50 FT-IR, ThermoScientific™, USA) with a wavelength range of 500 – 4000 cm^{-1} . Figure 2 illustrates the experimental methodology.

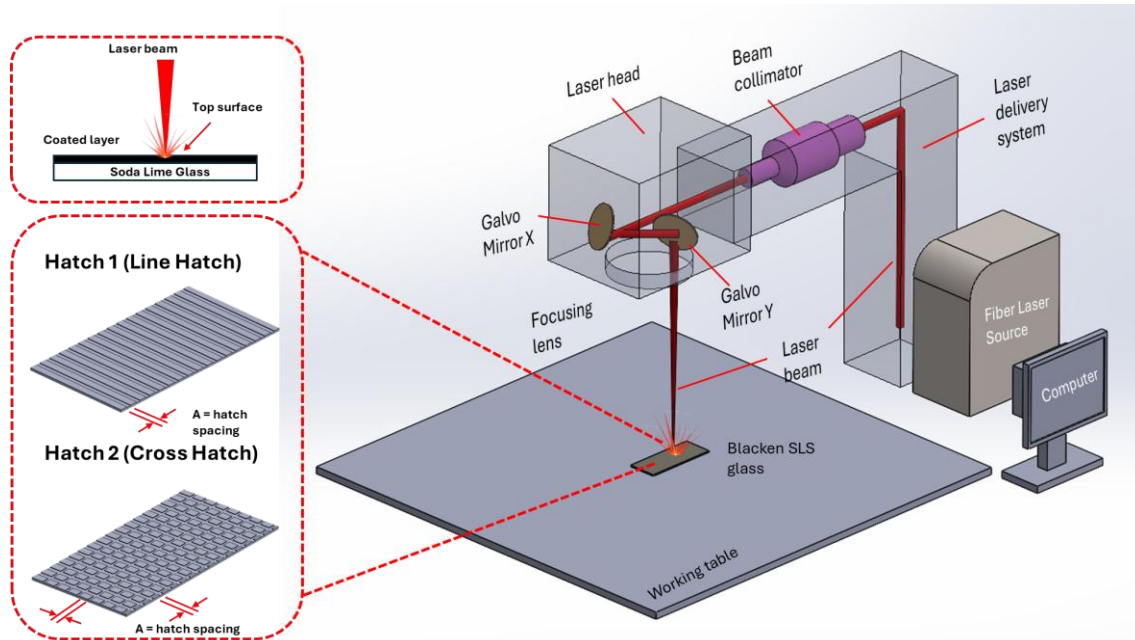


Figure 2 : Schematic illustration of the laser texturing process with variations on hatch pattern.

3.0 RESULTS AND DISCUSSION

3.1 Surface Wettability

The surface wettability of the modified sample showed drastic changes in water contact angle, particularly on samples textured with a 60 μm spacing, with three of these samples transformed to a hydrophobic state. Pristine glass exhibits a water contact angle of 33.89°, aligned with the result reported by Dinh et al. (2020) and Soldera et al. (2021); the transformation from hydrophilic to hydrophobic demonstrates the effectiveness of laser texturing in modifying the surface wettability of soda lime silica glass without the use of hazardous chemicals as a secondary process.

Figure 3 shows the average water contact angle for all eight modified glass samples. The highest recorded contact angle was 96.41°, achieved through laser texturing with a 60 μm spacing, line hatch pattern and operated at a laser fluence of 424.4 mJ/mm^2 . On the other hand, the lowest contact angle (37.19°) was recorded at a spacing of 500 μm with a line hatch pattern and a fluence of 212.2 mJ/mm^2 . These results indicated that the hatch spacing of 60 μm significantly altered the surface from hydrophilic to hydrophobic compared to larger spacings.

Working with hatch spacing of 60 μm creates a dense lasered area, covering nearly the entire surface compared to larger spacing. As more beam profiles interact with the material, the result is more textured topography than using larger hatch spacings. This produces surfaces with numerous microgrooves, removing more material and forming irregular patterns as shown in Figure 4(a). As the spacing increases, the proportion of microgroove regions as well as the sizes of the pit decrease leading to a more uniform and similar periodic structure as in Figure 4**Error! Reference source not found.**(b).

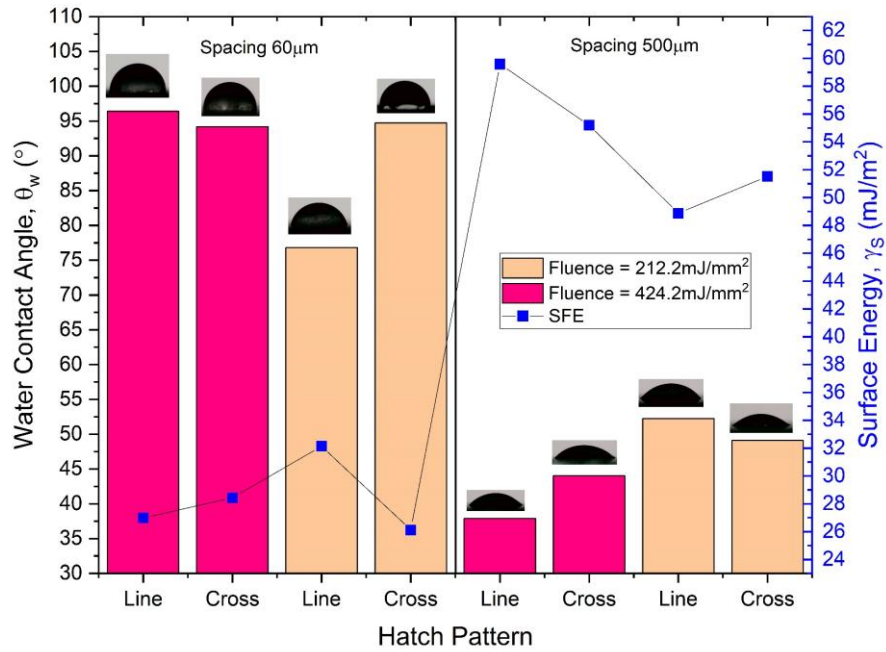


Figure 3: Surface wettability of modified glass using laser texturing technology.

Changes in surface wettability on different hatch spacing aligned with various researchers, who note that spacing interval has integral effects on modified glass wettability due to the transformation of surface topography (Cui et al., 2024; Dinh et al., 2020; Liu et al., 2024; Q. Wang et al., 2023; Zhou et al., 2024). These findings suggest that the formation of microgrooves on the laser-textured surface creates multiple air traps (Figure 5), preventing water penetration into the microgrooves (X. Li et al., 2023; Liao et al., 2023; Liu et al., 2024; Nguyen et al., 2021; Q. Wang et al., 2023). Denser microgrooves and deeper micro pits enhance the hydrophobicity of the surface, leading to a Cassie-Baxter non-wetting state; where the water droplets have difficulty penetrating the gaps. These miniature surface structures store air as a cushion layer between the glass substrate and water droplet (Liao et al., 2023).

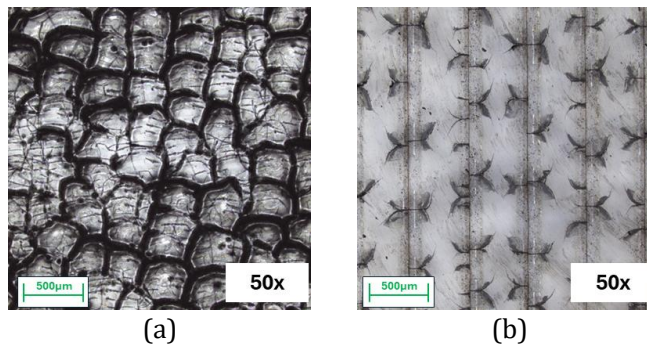


Figure 4: Comparison of microgroove density on laser textured glass; (a) 60 μm crosshatch spacing; (b) 500 μm line spacing.

In contrast, larger spacing intervals reduce the air-trapping effect, allowing water droplets penetrate the microgroove and stay pinned on the sample surface (Nguyen et al., 2021; Q. Wang et al., 2023). Reports from Lin et al. (2018), Q. Wang et al. (2023), Zhao et al. (2022) and Jing et al. (2022) concluded that the threshold value for hatch spacing ensures the transformation of surface wettability into more hydrophobic regions.

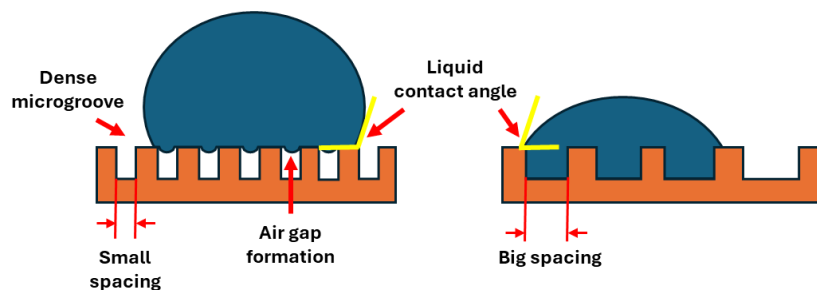
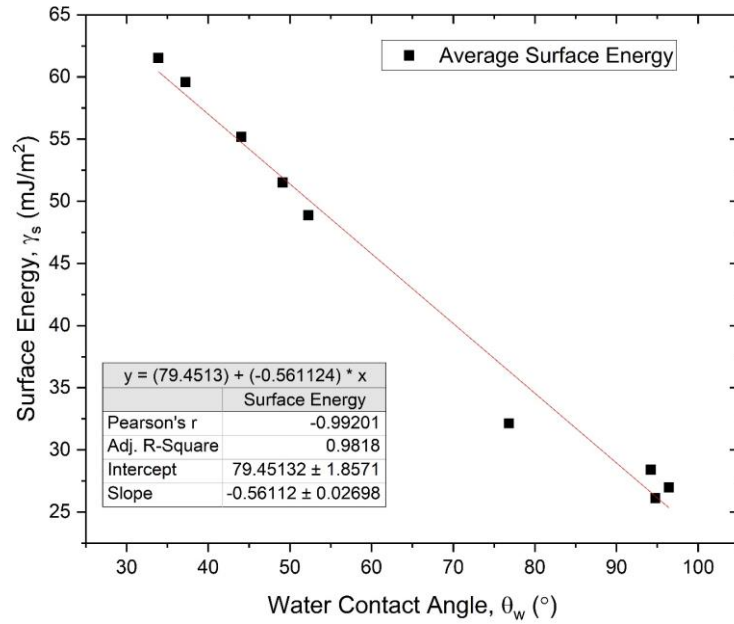


Figure 5: Formation of multiple air traps on high-dense microgrooves.

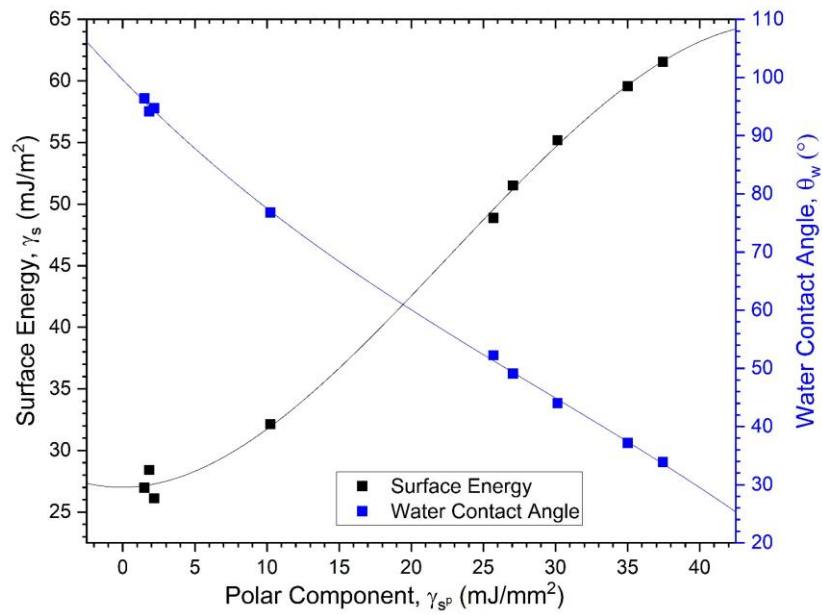
3.2 Surface Energy

A negative interaction between water contact angle and surface energy is evident in Figure 3. Surface energy is clustered in two segments; one for the 60 μm and one for the 500 μm spacing. A significant reduction in surface energy occurred in sample textured with smaller spacing compared to pristine glass, which measured at 64.54 mJ/m^2 (Hejda et al., 2010; Moreno Baqueiro Sansao et al., 2021). Texturing at 60 μm intervals reduced surface energy by approximately 35 mJ/m^2 (water contact angle, $\theta_w = 94.7^\circ$), while texturing at 500 μm resulted in a reduction of about 1.96 mJ/m^2 ($\theta_w = 37.2^\circ$). This negative interaction (Figure 6a) reflects the lower surface wettability due to the reduction in surface energy that prevents water droplets from adhering to the surface. This causes the water droplet to remain semispherical and prevents full penetration of the formed groove from the laser texturing process.

The reduction of polar energy components associated with the oxygen content in the modified glass contributed directly to lowering the surface energy, thus increasing the water contact angle, as illustrated in Figure 6b. Studies by Parvate et al. (2020), Sui et al. (2022) and Vieira et al. (2020) confirmed that the reduction of the polar energy component enhances the water-repellency effect. Since water is a polar molecule, reducing the polar molecule and polar energy inhibits water's ability to pin to the surface (Ahmad et al., 2018). Meanwhile, dispersive or non-polar components, which do not react with the oxygen content on the surface, exhibited only minor variations. Figure 7 displays the polar and dispersive components of surface energy for laser-modified soda lime silica glass.



(a)



(b)

Figure 6 : (a) Negative correlation between surface energy and water contact angle and (b) Interaction between polar components, surface energy and surface wettability.

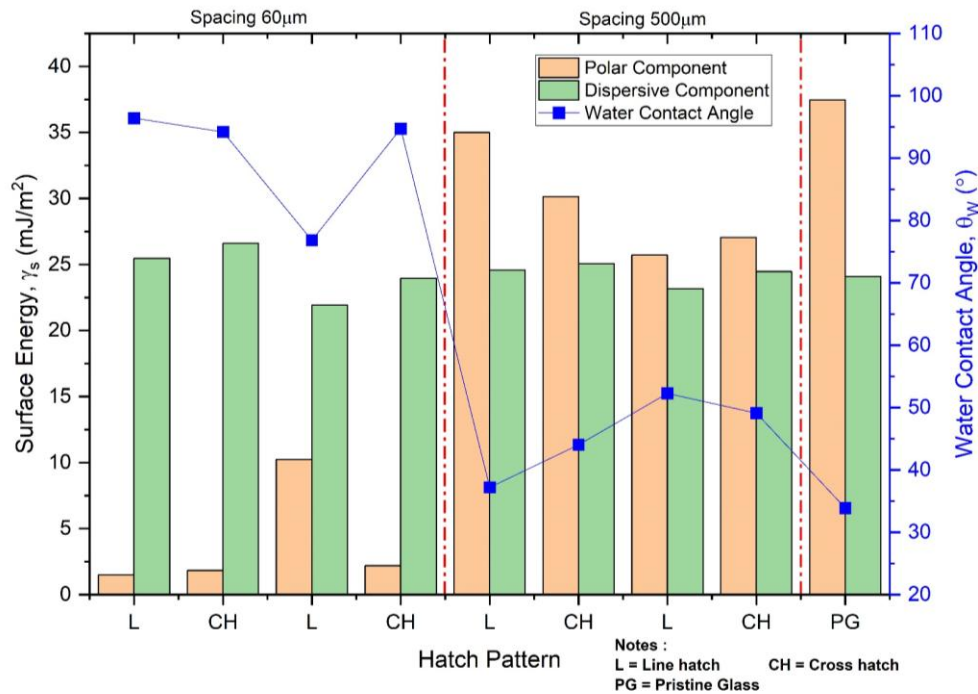


Figure 7 : Polar and dispersive components of surface energy for laser-textured glass.

3.3 Surface Topography

The surface topography was evaluated based on profile roughness, as described by the standard mentioned earlier. Figure 8 presents the measured values for Rz, Rv, Rp and Ra for modified samples with variations in laser texturing parameters. In general, all roughness values were higher while working with a spacing of 60 μm compared to 500 μm. The denser topography created by the smaller hatch spacing contributed to the higher roughness value, which in turn, influenced surface wettability. With more cavities formed, the air was stored in the grooves, creating an air cushion between the liquid and the solid substrate.

The result showed Rz values ranging from 23.31 μm to 45.46 μm when texturing with a 60 μm spacing; meanwhile, values ranged from 1.74 μm and 2.49 μm for samples processed with 500 μm spacing. These integral effects responded well with the theory mentioned by various authors, which concluded that larger spacing increases the water adhesion effect, thereby improving surface wettability (Arbain et al., 2024; Dinh et al., 2020; Lin et al., 2018; Ouchene et al., 2023; Yang et al., 2020). For instance, Lin et al. (2018) reported that a 30 μm spacing yielded a hydrophobic surface with chemical post-treatment on 1 mm thickness silica glass. Meanwhile, Liao et al. (2023) found that an optimal interval of 60 μm was needed to achieve hydrophobic effect on a commercial soda lime silica glass.

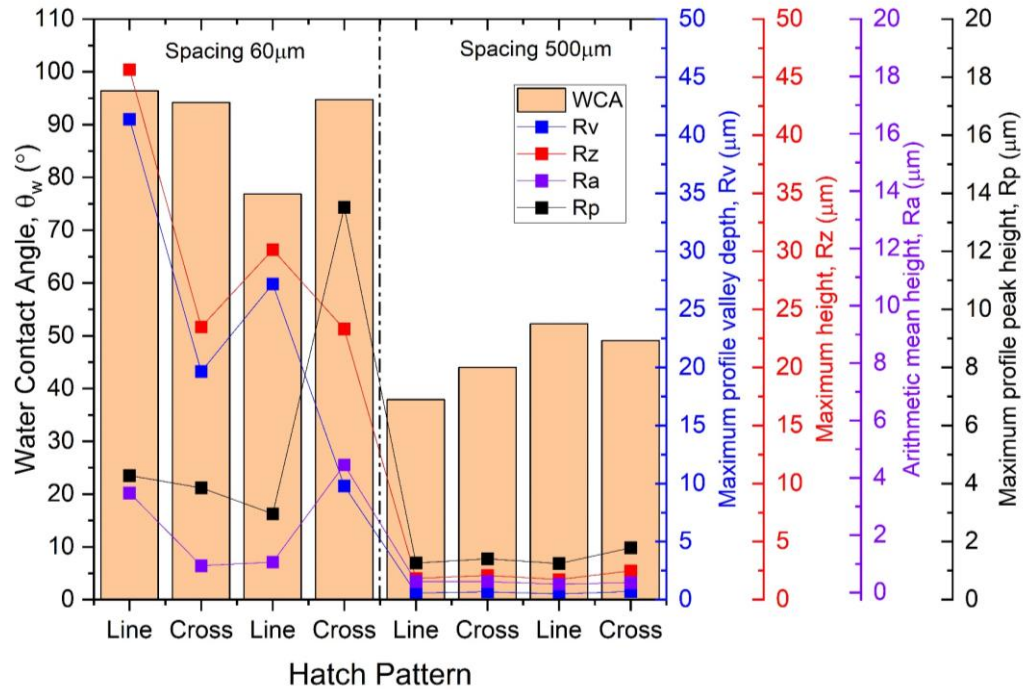


Figure 8: Profile roughness corresponding to water contact angle at different laser texturing parameters.

Figure 8 shows that an Ra threshold value of 1 μm significantly increases the wettability of soda lime silica glass, shifting it towards hydrophobic behaviour. The roughness range of 0.935-4.45 μm (at 60 μm spacing) responds to the higher water contact angles. In contrast, an Ra value below 0.385 μm results in minimal wettability transformation on the modified glass. These findings support the hypothesis that surface roughness profiles impact the wettability of laser-textured glass (K. Li et al., 2022; X. Li et al., 2023; Ouchene et al., 2023).

The range of Rz value in the current results aligns with previous works, as modified surface responses can vary significantly. For instance, quartz coated with perfluorodecyltriethoxysilane experienced a reduction of water contact angle when microgroove depth exceeds 3.5 μm (Zhao et al., 2022). As for ultra-white glass, a microgroove depth greater than 26 μm is required to alter surface wettability (Jing et al., 2022). Additionally, a 1065 nm picosecond laser can reduce the surface wettability of 1mm thickness quartz coated with polytetrafluoroethylene films where Rz needs to exceed 28.5 μm (Gao et al., 2022).

The relationship between laser texturing parameters and surface topography is illustrated in Figure 9. A similar trend occurred for peak and valley formation as smaller hatch spacing generates a slightly higher value indicating that a rougher profile was produced. This experimental work also recorded a positive interaction between laser fluence and surface topography. Pulsing energy affects the formation of microgrooves as bigger pulse energy creates deeper grooves. In terms of hatch pattern, both selected patterns do not greatly influence the formation of microgrooves as these parameters depend on factor A (hatch spacing) and factor B

(laser fluence). Figure 10 compares stacking profiles of microgroove formation at 60 μm and 500 μm spacing, emphasizing variations due to different laser processing parameters.

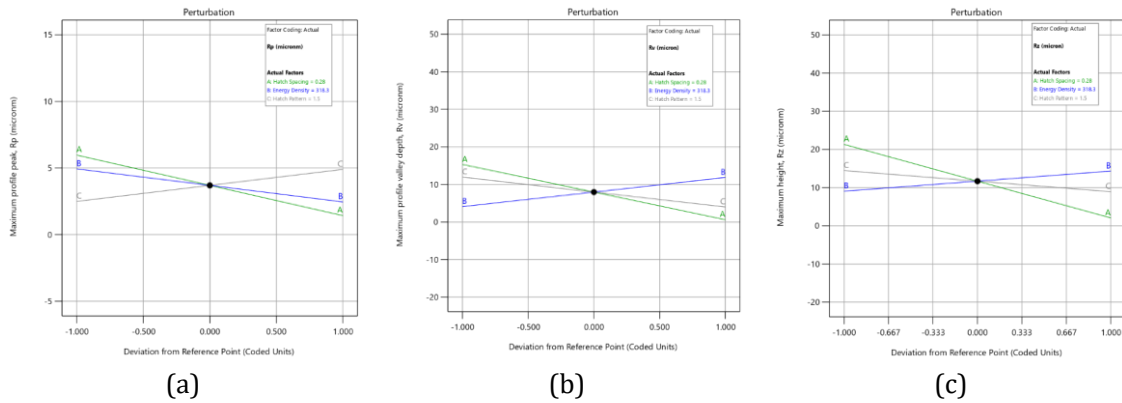


Figure 9: Relationship between surface topography and laser texturing parameters; (a) maximum profile peak height, Rp (b) maximum profile valley depth, Rv; (c) maximum profile height, Rz.

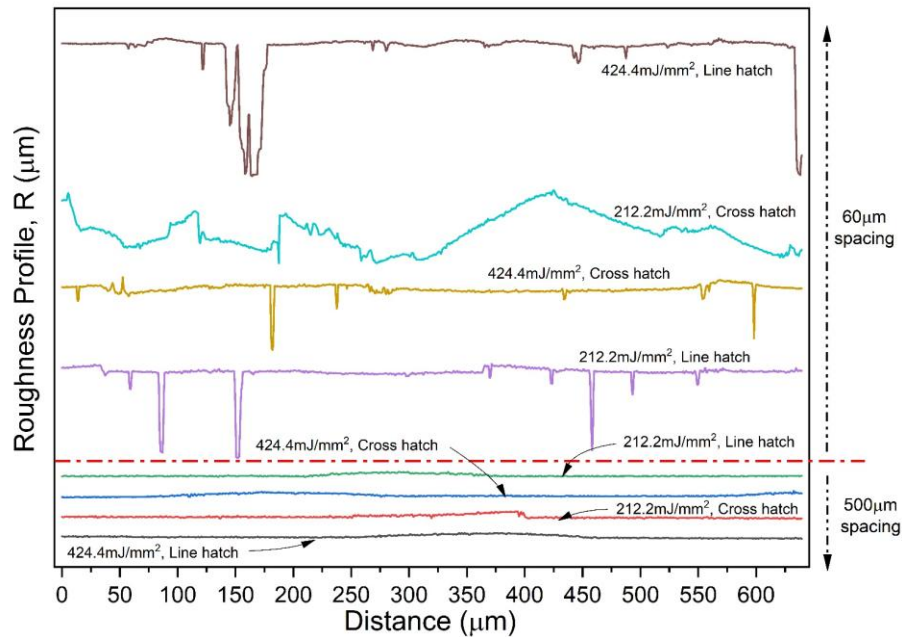


Figure 10: Stacking roughness profile comparison for laser textured soda lime silica glass with different laser processing parameters.

Correlation between glass surface parameters and surface energy reveals that quadratic interaction for these parameters in determining the transformation of surface wettability (Figure 11). This result aligned with Young’s Model and the results from various research as mentioned in the previous section. The reduction of surface energy depends on the changes in surface topography and chemical composition (Gunerhan & Genc Oztoprak, 2023; Mishra et al., 2023).

Notably, the sample with a high value of roughness exhibited lower surface energy, which correlated with higher water contact angle. The reduction of surface energy is likely due to less contact surface between the glass and water droplet with the support of the depletion of chemical composition that has a water attraction effect.

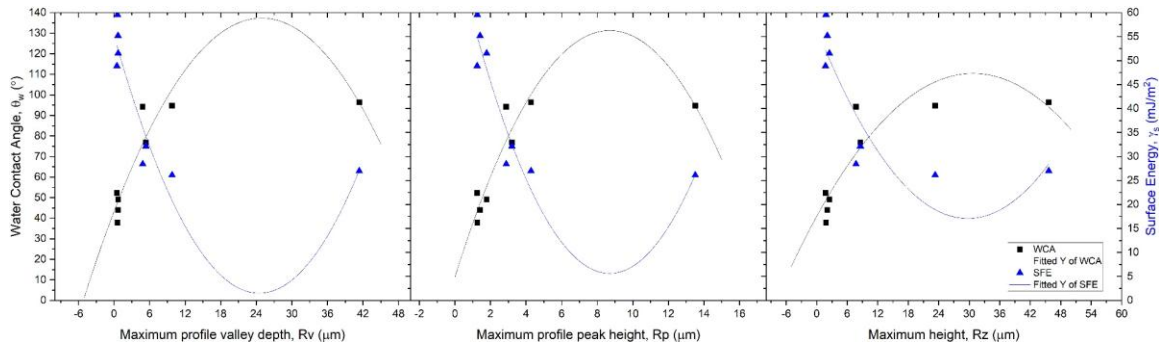


Figure 11: Correlation between surface energy and glass surface parameters.

3.4 Surface Morphology

Surface morphology is a critical factor in determining surface wettability, as it affects both surface roughness and chemistry (Ibrahim et al., 2022; Peethan et al., 2023). Laser processing of soda lime silica glass resulted in rapid changes to the surface chemistry due to the thermal effect, which influenced surface energy (Arbain et al., 2024; Gunerhan & Genc Oztoprak, 2023; Hong et al., 2024; Jothi Prakash & Prasanth, 2021; Mishra et al., 2023). Changes in composition and molecule bonding on the modified glass surface reacted to the surface wettability can be seen in Figure 12 and Figure 13.

From ATR-FTIR analysis in Figure 12, a reduction of Si-O-Si peaks at 764 and 1040 cm^{-1} was detected. These respond to a decrease in the SiO_2 asymmetrical and symmetrical stretching vibration thus lowering the bonding intensity (Arellano-Galindo et al., 2022; Junaidi et al., 2017; Kumar et al., 2023; Z. H. Zhang et al., 2018; Zhong et al., 2022). As SiO_2 bonding intensity is related to hydrophilic properties, reducing this bond facilitates the transformation to a hydrophobic state.

Additionally, a reduction in oxygen bonding at 3336 cm^{-1} wavelength represents a decrement in the hydroxyl functional group. This reduction occurred due to localized heating from the laser beam that modified the bond and reduced the intensity of the glass hydroxyl group. Since the hydroxyl group is crucial in glass hydrophilicity, its reduction leads to a more hydrophobic surface (Aono et al., 2016; Deng et al., 2023; Khan et al., 2021; Ouchene et al., 2023; Yusuf et al., 2022; Z. H. Zhang et al., 2018). This theory was used in chemical processing as a secondary process to remove the exposed OH functional group on the glass surface thus creating a superhydrophobic glass.

The reduction in oxygen content of modified glass influences their hydrophobicity. Figure 13 presents the percentage composition of laser-textured soda lime silica glass from EDXs analysis. A significant reduction of oxygen content is observed on samples with high water contact angles. Although glass is composed primarily of oxide-based material, the abundance of oxygen content is still available as this atom bonded with other natural elements as non-bridging oxygen. The reduction of hydroxyl groups, which contain oxygen is further confirmed by ATR-FTIR results.

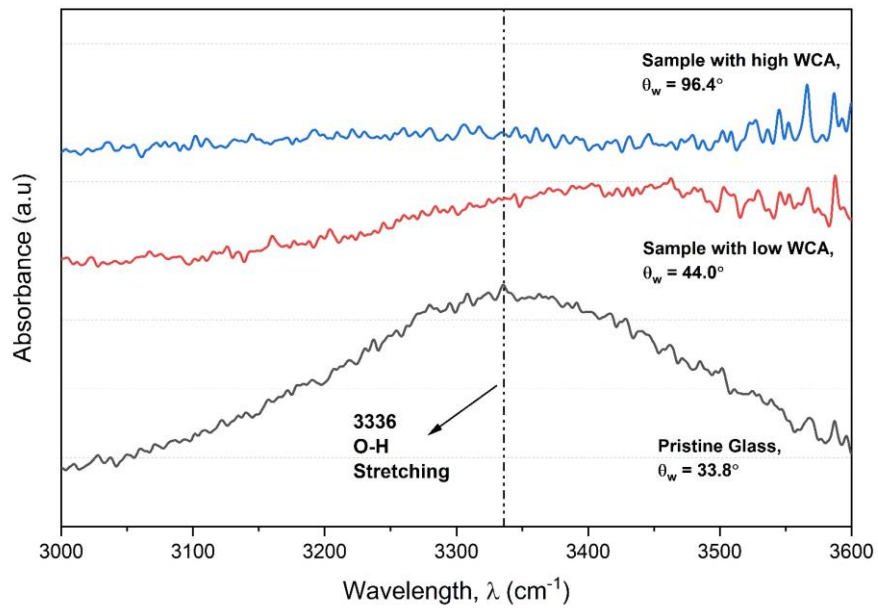
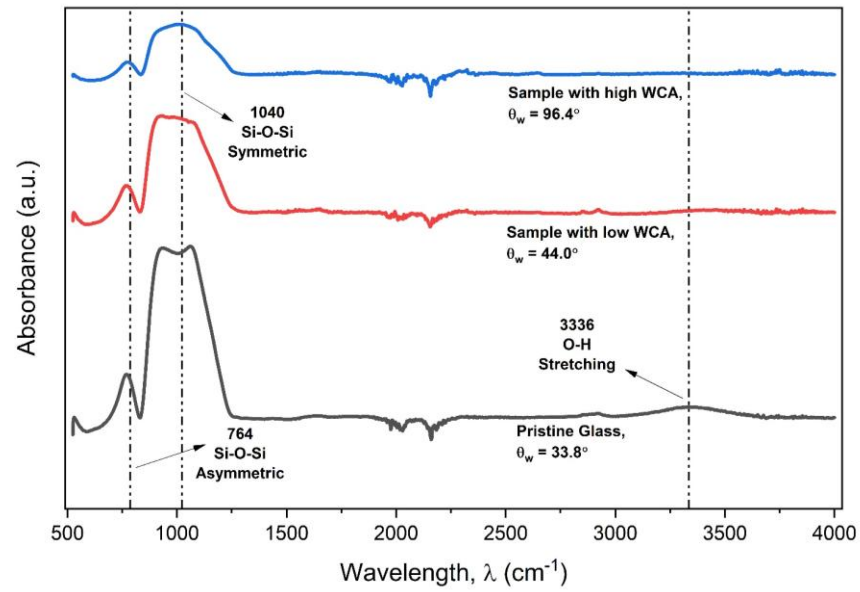


Figure 12 : ATR-FTIR spectra in the range of 500 – 4000 cm^{-1} for pristine glass and laser textured glass.

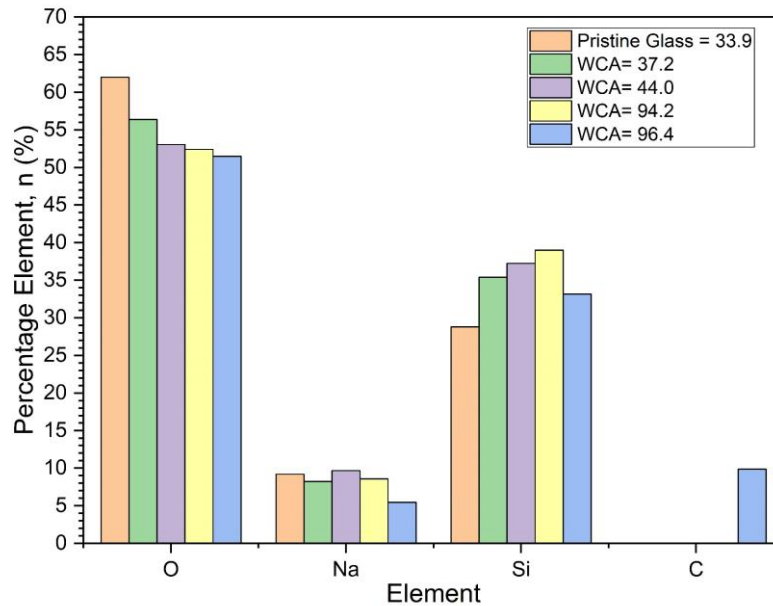


Figure 13: Changes in element composition of modified glass.

The interaction between oxygen content and surface wettability in laser-textured soda lime silica glass is illustrated in Figure 14. A negative correlation is observed between oxygen content with water contact angle, with an inverse effect on surface energy. Oxygen is an ionic polar element that plays a significant role in the interaction between the glass surface and water droplet. Joy & Kietzig (2023) suggested that reduction in polar energy especially on hydroxyl ions reduces the surface polarity thus creating a more hydrophobic surface. The observed reduction in polar energy through laser texturing is noteworthy, as most research has relied on fluorinated-based compounds as low surface energy agents due to their non-polar chemistry (Alves & Sousa, 2024). Additionally, a slight increase in the Si percentage content, as shown in Figure 13, results from the reduced oxygen content in the Si-O-Si bond.

Visual inspection of the modified glass showed that certain parameters led to microcracks formation (as in Table 4), with chipping particularly noticeable along the laser beam path. Multiple cracks with heavy concentric and radial propagation were observed on the samples with 60 μm spacing attributed to unresolved heat and thermal differences on the glass surface. A similar pattern of crack formation was observed in samples exposed to either 212.2 mJ/mm^2 or 424.4 mJ/mm^2 , as illustrated in Table 4. Despite the laser pulse energy within the threshold value of soda lime silica glass, operating at 60 μm spacing introduced uncontrolled compressive stress and tensile stress at both the surface and subsurface levels (Najwa et al., 2024; Shin & Nam, 2020).

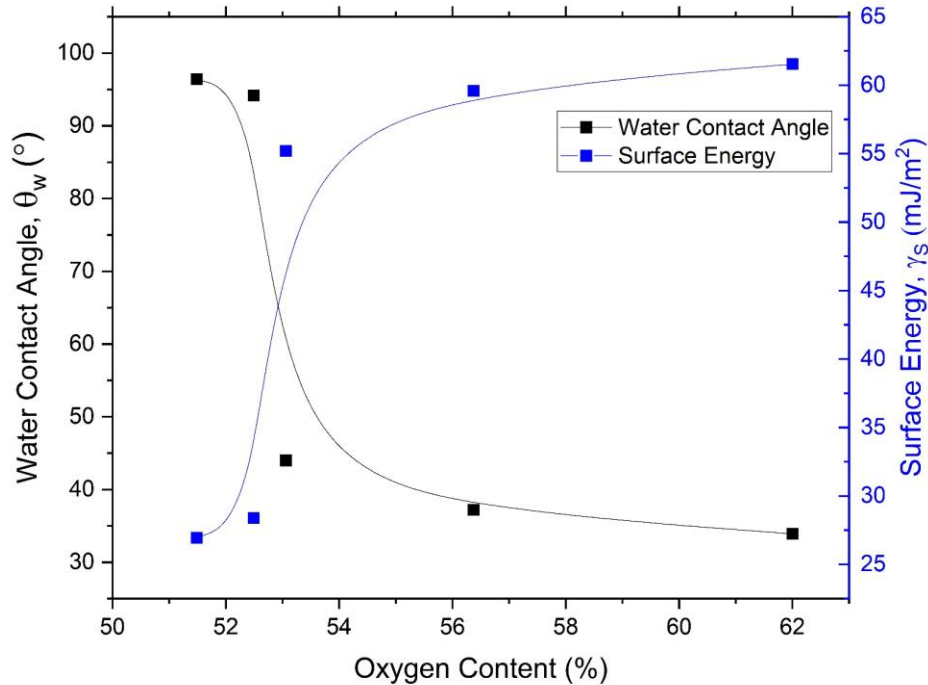
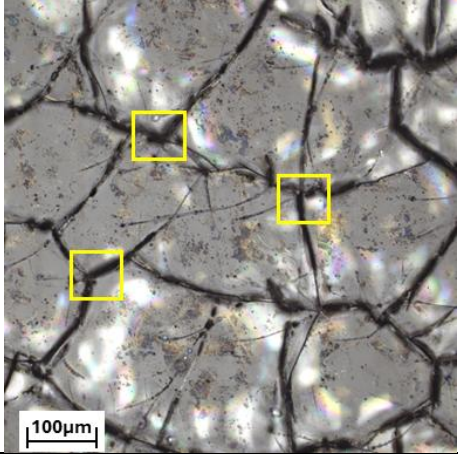
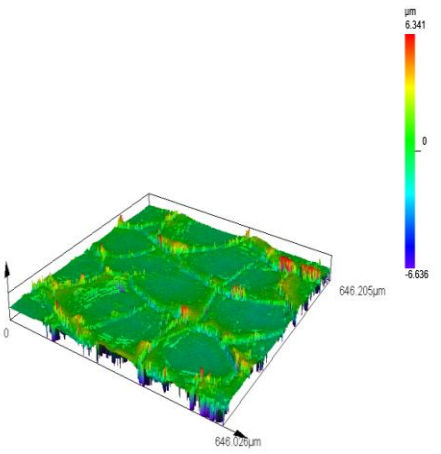
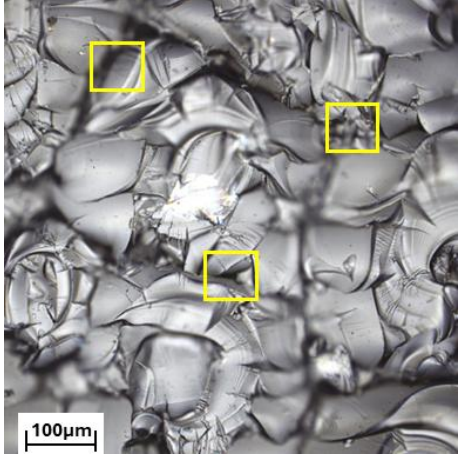
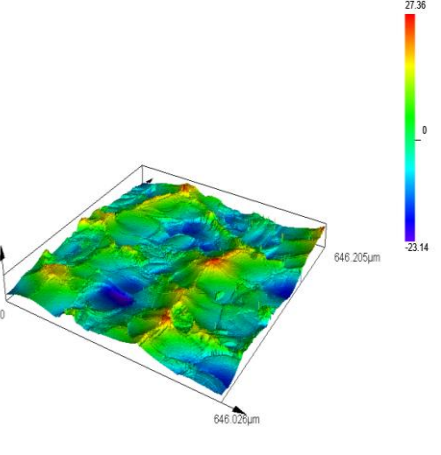


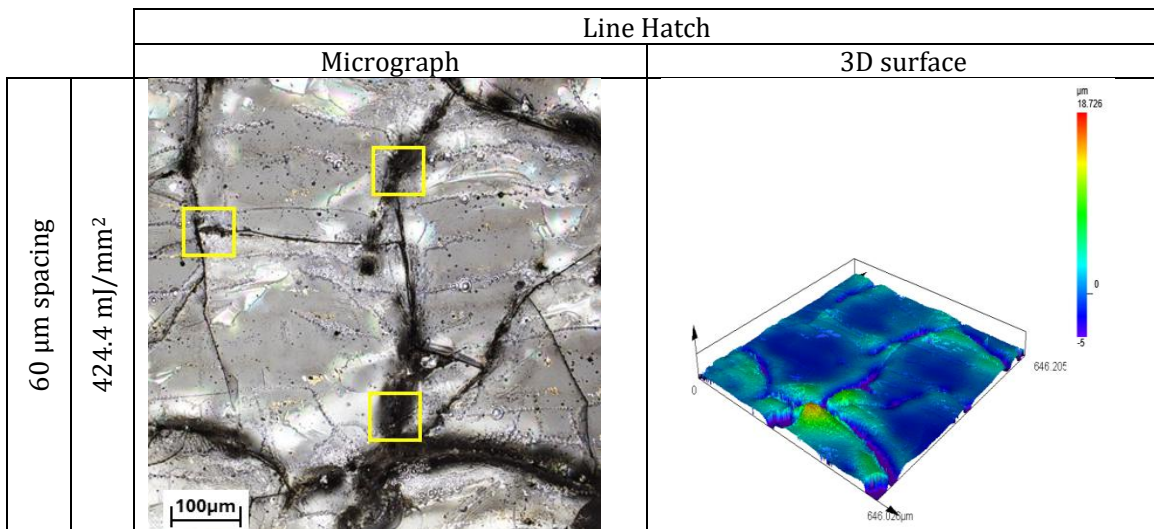
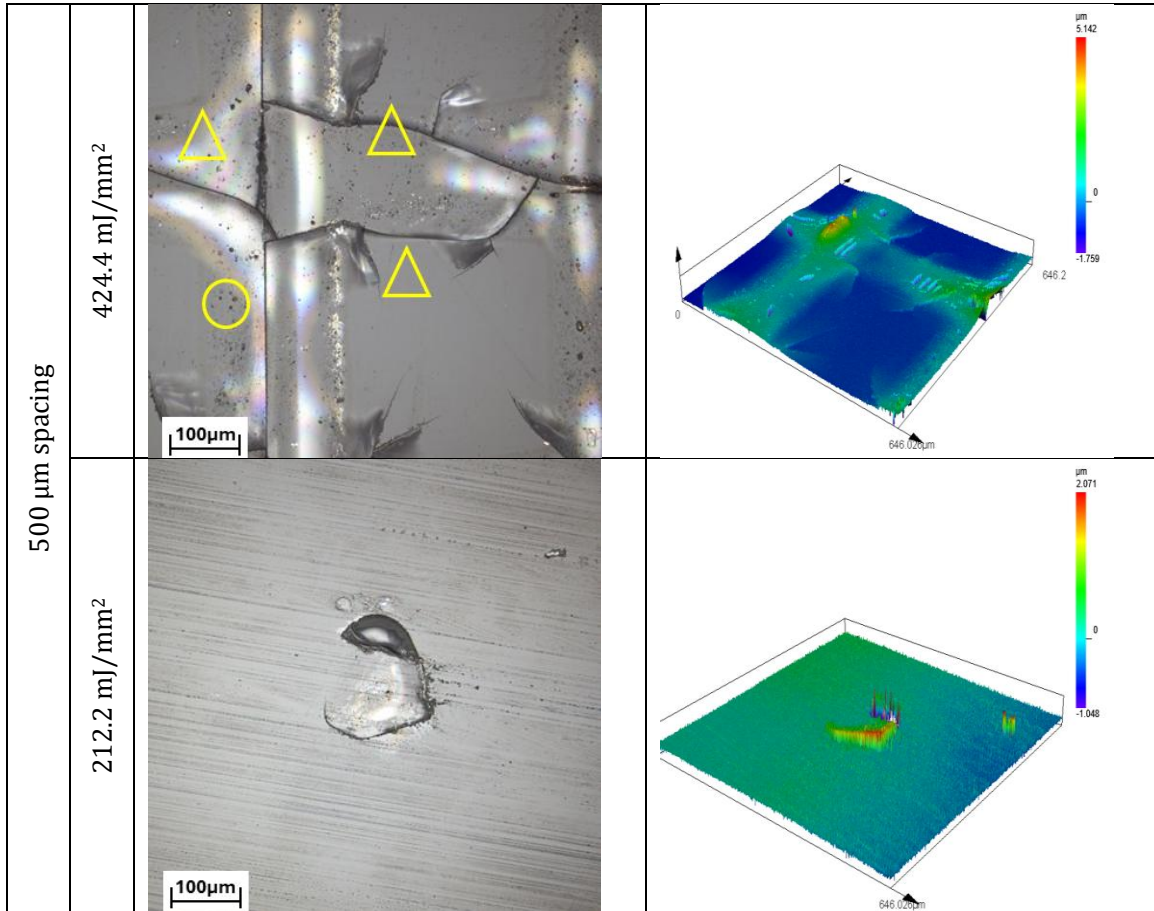
Figure 14: Interaction between surface wettability and oxygen content of soda lime silica glass.

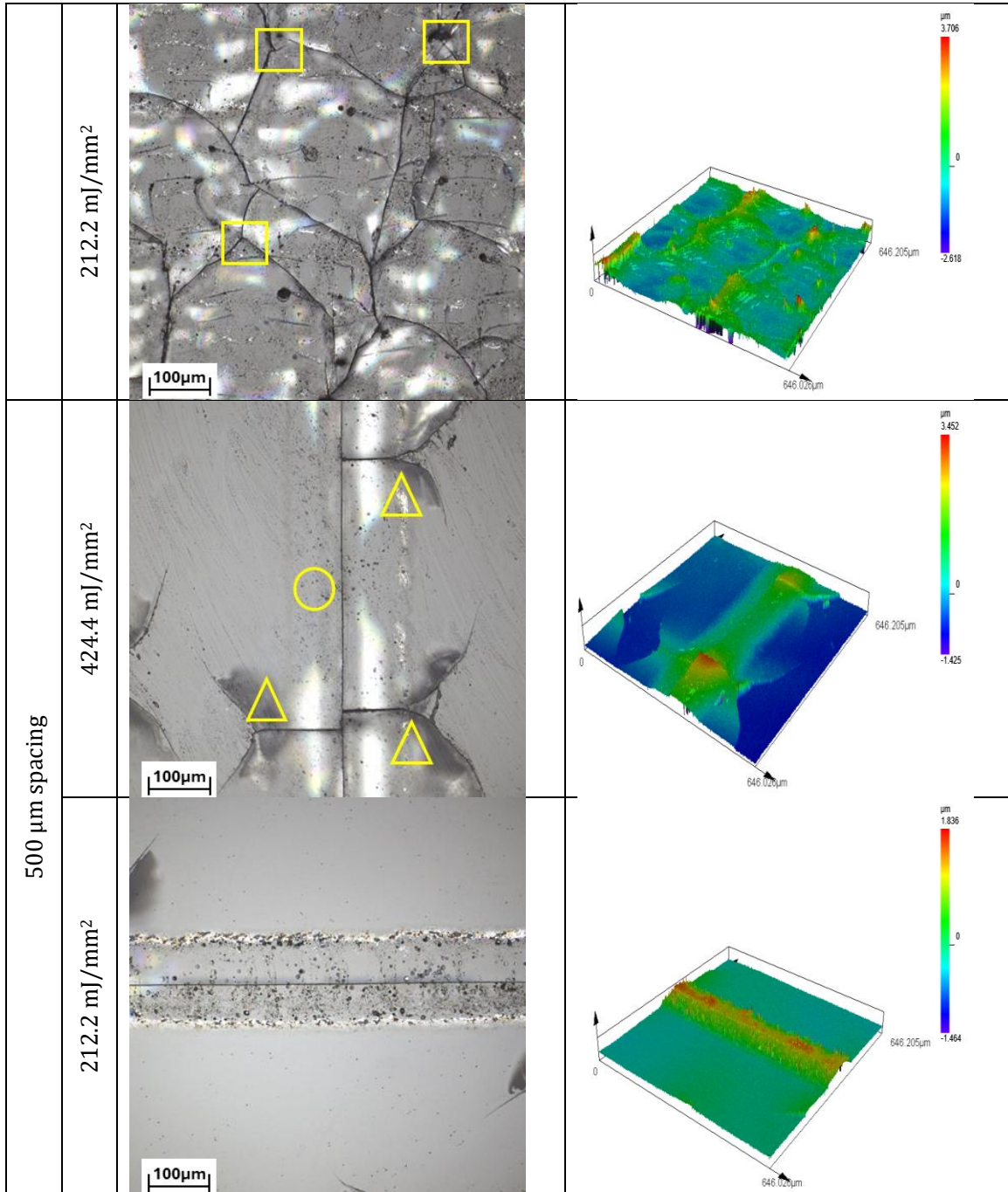
Meanwhile, only a small microcrack occurred at the laser beam path with nanoscale radial crack propagation toward the non-beam area at 500 μm spacing with 424.4 mJ/mm^2 laser fluence. These cracks occurred due to the high thermal sensitivity of glass, especially soda lime silica glass ($9 \times 10^{-6}/\text{K}$) which is higher compared to other types of glass. Thermal expansion and contraction strains induced by laser plasma resulted in the formation of cracking (Nategh et al., 2021; Pan et al., 2017). Observation in Figure 15 shows that the formation and size of bubbles within the laser-textured glass are affected by laser irradiation and hatch spacing. The presence of bubble formation suggests vaporization, which is a primary source of crack formation (Shin, 2019). A crack-free textured glass was found at samples 212.2 mJ/mm^2 with 500 μm spacing as the heat from the laser beam was effectively absorbed by the modified glass, minimizing thermal differences due to the larger spacing.

Although microcrack from laser processing on glass has been a major challenge in modifying glass wettability, it can resolve by reducing the energy density and increasing the hatch spacing. Concurrently, minimum energy and accurate roughness are required to produce microgrooves and texture on the glass.

Table 4: SEM images and 3D topography of laser irradiated areas with variation in hatch pattern, spacing and laser fluence. The triangle in the figures indicates the cracks propagation across the scanning direction, the circle denotes the cracks propagation along the scan direction while the square represents a combination of radial and concentric cracks.

		Cross Hatch	
		Micrograph	3D surface
60 μm spacing	424.4 mJ/mm ²		
	212.2 mJ/mm ²		





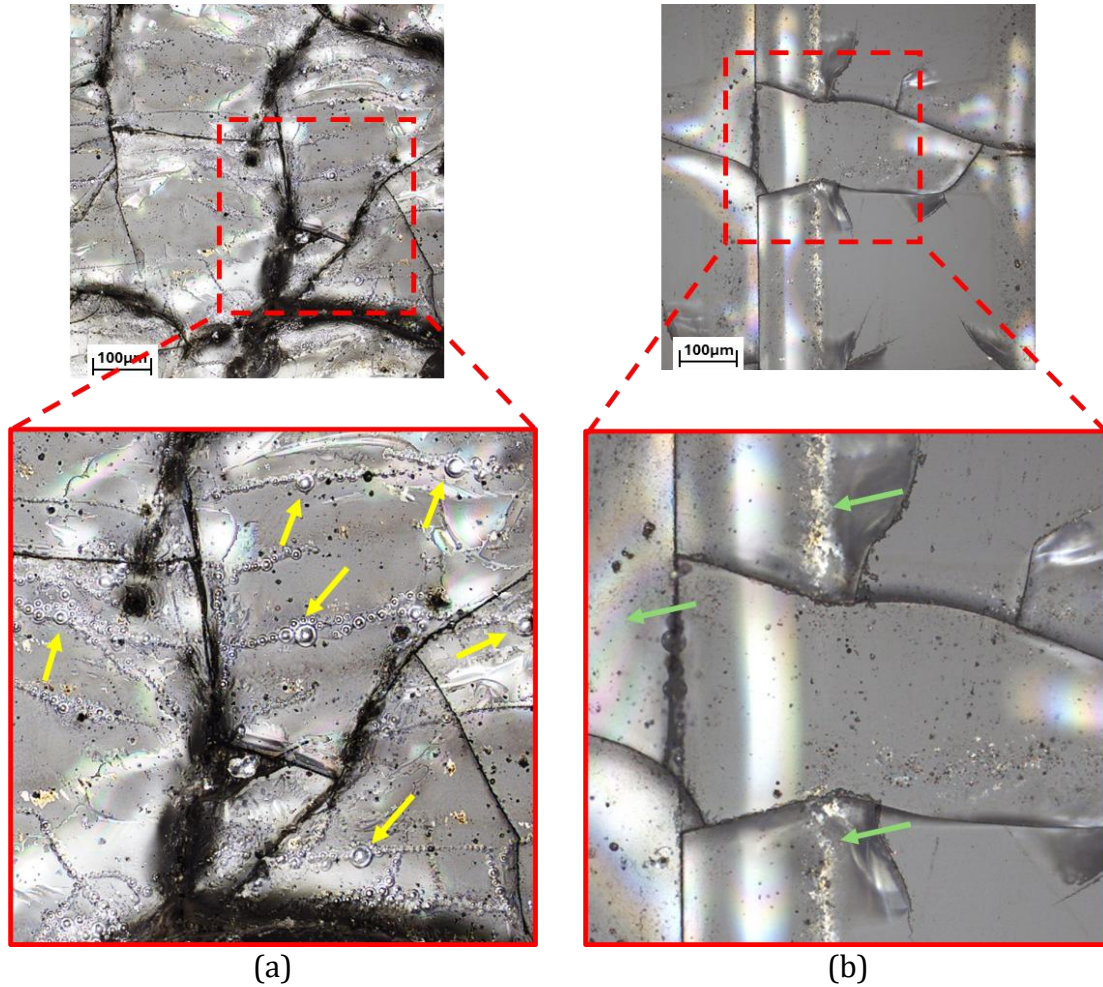


Figure 15: Bubbles formation at crack propagation area with yellow arrow micro bubbles and green arrow denotes nano sized bubbles; (a) 60 μm cross hatch spacing; (b) 500 μm line spacing.

CONCLUSIONS

In this work, the modification of soda lime silica glass wettability without using any hazardous chemical as a secondary process was investigated. The discovery using the laser texturing process reveals that changes in surface topography and surface chemistry have a significant effect on the glass wettability. Surface wettability was evaluated as a response to variations of hatch spacing, pattern and laser fluence. Surface wettability was found to interact with surface topography and surface chemistry. On the basis of current findings, it can be recognized that reducing the hatch spacing significantly affects the surface topography and surface chemistry thus transforming hydrophilic soda lime silica glass into hydrophobic properties.

A higher water contact angle was recorded while working at smaller spacing as this influenced the surface topography, surface energy and surface chemistry. The formation of multiple microgrooves changes the surface energy and surface chemistry. With the ability to achieve up to

96° water contact angle, a bright prospect on tuning the wettability of glass using laser processing method.

In future, a study on light transmissibility is recommended to ensure the transparency of glass after modifying its wettability for applications like window panels and windscreens. Tailoring wettability at dedicated areas on the substrate for functional applications such as high-rise building windows, vehicle side mirrors and solar panels could be beneficial to extend the basic function of glass nowadays. Overall, this work paved the way for modifying hydrophilic glass to a desired wettability without the usage of hazardous chemicals and adaptation to new emerging technologies.

ACKNOWLEDGEMENTS

The authors gratefully acknowledge the financial support from the Ministry of Higher Education Malaysia under the Fundamental Research Grant Scheme FRGS/1/2021/TK0/UMP/02/48 (University reference: RDU210145) and Universiti Malaysia Pahang Al-Sultan Abdullah. The authors also thank Mr. Abdul Rahman Rosman and Mr. Muhamad Haikal Asyraf Md Raizi for their contribution to this study. The authors also would like to acknowledge the machine and research facilities provided by Kolej Kemahiran Tinggi MARA Kuantan.

REFERENCES

- Ahmad, D., van den Boogaert, I., Miller, J., Presswell, R., & Jouhara, H. (2018). Hydrophilic and hydrophobic materials and their applications. *Energy Sources, Part A: Recovery, Utilization and Environmental Effects*, 40(22), 2686–2725. <https://doi.org/10.1080/15567036.2018.1511642>
- Alves, D. F., & Sousa, J. P. S. (2024). Fluorine-free approaches to impart photovoltaic systems with self-cleaning and anti-icing features. *Journal of Coatings Technology and Research*. <https://doi.org/10.1007/s11998-024-00936-1>
- Aono, Y., Hirata, A., & Tokura, H. (2016). Non-textured laser modification of silica glass surface: Wettability control and flow channel formation. *Applied Surface Science*, 371, 530–537. <https://doi.org/10.1016/j.apsusc.2016.03.040>
- Arbain, N. A., Zini, N. H. M., Anuar, F. S., Abdollah, M. F. Bin, & Rosley, M. I. F. (2024). Wettability characterization of 3D printed polymer membranes with candle soot coating. *Jurnal Tribologi*, 40(October 2023), 148–163.
- Arellano-Galindo, L. G., Reynosa-Martínez, A. C., Gaitán-Arévalo, J. R., Valerio-Rodríguez, M. F., Vargas-Gutiérrez, G., & López-Honorato, E. (2022). Superhydrophobic to superhydrophilic wettability transition of functionalized SiO₂ nanoparticles. *Ceramics International*, 48(15), 21672–21678. <https://doi.org/10.1016/j.ceramint.2022.04.137>
- Bakhtiari, N., Azizian, S., & Jaleh, B. (2022). Hybrid superhydrophobic/hydrophilic patterns deposited on glass by laser-induced forward transfer method for efficient water harvesting. *Journal of Colloid and Interface Science*, 625, 383–396. <https://doi.org/10.1016/j.jcis.2022.06.039>
- Cui, H., Teng, C., Zhao, Y., Wang, P., Guo, Y., & Qi, X. (2024). Durable self-cleaning antireflective and antifog Al micro-nano structure on glass by laser marker ablation. *Optical Materials*, 147(December 2023), 114675. <https://doi.org/10.1016/j.optmat.2023.114675>

- Deng, Y., Li, Z., Rao, S., Zheng, H., Huang, X., Liu, Q., Wang, D., & Lu, H. (2023). Mechanism for the effects of surface chemical composition and crystal face on the wettability of α -quartz surface. *Applied Surface Science*, 633(March), 157559. <https://doi.org/10.1016/j.apsusc.2023.157559>
- Ding, C. F., Li, L., & Young, H. T. (2020). Laser-induced backward transfer of conducting aluminum doped zinc oxide to glass for single-step rapid patterning. *Journal of Materials Processing Technology*, 275(August 2019), 116357. <https://doi.org/10.1016/j.jmatprotec.2019.116357>
- Dinh, T.-H., Ngo, C.-V., & Chun, D.-M. (2020). Direct laser patterning for transparent superhydrophobic glass surfaces without any chemical coatings. *Applied Physics A*, 126(6), 462. <https://doi.org/10.1007/s00339-020-03653-9>
- Gao, J., Wu, Y., Zhang, Z., Zhao, D., Zhu, H., Xu, K., & Liu, Y. (2022). Achieving amorphous micro-nano superhydrophobic structures on quartz glass with a PTFE coating by laser back ablation. *Optics and Laser Technology*, 149(January), 107927. <https://doi.org/10.1016/j.optlastec.2022.107927>
- Goswami, A., Pillai, S. C., & McGranaghan, G. (2021). Surface modifications to enhance dropwise condensation. *Surfaces and Interfaces*, 25(March), 101143. <https://doi.org/10.1016/j.surfin.2021.101143>
- Gunerhan, A., & Genc Oztoprak, B. (2023). Production of Super-Hydrophobic Al₂O₃-TiO₂ Surfaces by Using Nanosecond Fiber Laser. *Journal of Materials Engineering and Performance*. <https://doi.org/10.1007/s11665-023-08338-x>
- Hejda, F., Solař, P., & Kousal, J. (2010). Surface Free Energy Determination by Contact Angle Measurements – A Comparison of Various Approaches. *WDS'10 Proceedings of Contributed Papers*, 3, 25–30.
- Hong, X., Zheng, Z., & Gao, Y. (2024). Construction of Robust Hierarchical Micro-nanostructure by Laser Irradiation and Hydrothermal Treatment on Titanium Alloy for Superhydrophobic and Slippery Surfaces. *Journal of Materials Engineering and Performance*, 33(4), 1885 – 1897. <https://doi.org/10.1007/s11665-023-08100-3>
- Ibrahim, S. H., Wejrzanowski, T., Przybyszewski, B., Kozera, R., García-Casas, X., & Barranco, A. (2022). Role of Surface Topography in the Superhydrophobic Effect—Experimental and Numerical Studies. *Materials*, 15(9), 1–14. <https://doi.org/10.3390/ma15093112>
- Jing, X., Xia, Y., Chen, F., Yang, C., Yang, Z., & Jaffery, S. H. I. (2022). Preparation of superhydrophobic glass surface with high adhesion. *Colloids and Surfaces A: Physicochemical and Engineering Aspects*, 633(P2), 127861. <https://doi.org/10.1016/j.colsurfa.2021.127861>
- Jothi Prakash, C. G., & Prasanth, R. (2021). Approaches to design a surface with tunable wettability: a review on surface properties. *Journal of Materials Science*, 56(1), 108–135. <https://doi.org/10.1007/s10853-020-05116-1>
- Joy, N., & Kietzig, A. M. (2023). Role of machining and exposure conditions on the surface chemistry modification of femtosecond laser-machined copper surfaces. *Surfaces and Interfaces*, 37(October 2022), 102657. <https://doi.org/10.1016/j.surfin.2023.102657>
- Junaidi, M. U. M., Azaman, S. A. H., Ahmad, N. N. R., Leo, C. P., Lim, G. W., Chan, D. J. C., & Yee, H. M. (2017). Superhydrophobic coating of silica with photoluminescence properties synthesized from rice husk ash. *Progress in Organic Coatings*, 111(March), 29–37. <https://doi.org/10.1016/j.porgcoat.2017.05.009>
- Khan, S. A., Ganeev, R. A., Boltaev, G. S., & Alnaser, A. S. (2021). Wettability modification of glass surfaces by deposition of carbon-based nanostructured films. *Fullerenes, Nanotubes and Carbon Nanostructures*, 29(8), 576–587. <https://doi.org/10.1080/1536383X.2021.1871897>

- Kumar, S., Singh, K., & Kumar, D. (2023). Asymmetric SiO₂ structural units modification by Li₂O and their effect on optical and mechanical properties of soda lime silicate glasses. *Ceramics International*, 49(16), 26302–26312. <https://doi.org/10.1016/j.ceramint.2023.05.143>
- Li, K., Myers, N., Bishop, G., Li, Y., & Zhao, X. (2022). Study of surface wettability on fused silica by ultrafast laser-induced micro/nano-surface structures. *Journal of Manufacturing Processes*, 79(April), 177–184. <https://doi.org/10.1016/j.jmapro.2022.04.035>
- Li, X., Zhang, G., Xu, X., Zhao, G., Liu, Y., & Yin, S. (2023). Fabrication of superhydrophobic surfaces on a glass substrate via hot embossing. *Ceramics International*, 49(16), 26338–26347. <https://doi.org/10.1016/j.ceramint.2023.05.169>
- Liao, K., Wang, W., Mei, X., Zhao, W., Yuan, H., Wang, M., & Wang, B. (2023). Stable and drag-reducing superhydrophobic silica glass microchannel prepared by femtosecond laser processing: Design, fabrication, and properties. *Materials and Design*, 225, 111501. <https://doi.org/10.1016/j.matdes.2022.111501>
- Lin, Y., Han, J., Cai, M., Liu, W., Luo, X., Zhang, H., & Zhong, M. (2018). Durable and robust transparent superhydrophobic glass surfaces fabricated by a femtosecond laser with exceptional water repellency and thermostability. *Journal of Materials Chemistry A*, 6(19), 9049–9056. <https://doi.org/10.1039/c8ta01965g>
- Liu, S., Sun, C., Zhang, K., Geng, Y., Yu, D., & Wang, C. (2024). Fog collection efficiency of superhydrophobic surfaces with different water adhesion prepared by laser grid texturing. *Optics and Laser Technology*, 172. <https://doi.org/10.1016/j.optlastec.2023.110523>
- Luo, M., Sun, X., Zheng, Y., Cui, X., Ma, W., Han, S., Zhou, L., & Wei, X. (2023). Non-fluorinated superhydrophobic film with high transparency for photovoltaic glass covers. *Applied Surface Science*, 609(October 2022), 155299. <https://doi.org/10.1016/j.apsusc.2022.155299>
- Mishra, V., Gedeon, O., & Gavenda, T. (2023). Surface and subsurface alterations in freshly fractured and corroded soda-lime float glass. *Journal of the American Ceramic Society*, February. <https://doi.org/10.1111/jace.19047>
- Moreno Baqueiro Sansao, B., Kellar, J. J., Cross, W. M., Schottler, K., & Romkes, A. (2021). Comparison of surface energy and adhesion energy of surface-treated particles. *Powder Technology*, 384, 267–275. <https://doi.org/10.1016/j.powtec.2021.02.029>
- Mulko, L., Soldera, M., & Lasagni, A. F. (2022). Structuring and functionalization of non-metallic materials using direct laser interference patterning: A review. *Nanophotonics*, 11(2), 203–240. <https://doi.org/10.1515/nanoph-2021-0591>
- Najwa, K. A. N., Najihah, Z., Aqida, S. N., Ismail, I., & Salwani, M. S. (2024). Laser Texturing of Soda Lime Glass Surface for Hydrophobic Surface in Wenzel State. *International Journal of Automotive and Mechanical Engineering*, 21(1), 10968–10980. <https://doi.org/10.15282/ijame.21.1.2024.02.0848>
- Nategh, S., Missinne, J., Vijverman, P., Van Steenberge, G., & Belis, J. (2021). Effect of ultrashort laser-induced surface flaws on architectural glass strength. *Construction and Building Materials*, 295. <https://doi.org/10.1016/j.conbuildmat.2021.123590>
- Nguyen, H. H., Tieu, A. K., Wan, S., Zhu, H., Pham, S. T., & Johnston, B. (2021). Surface characteristics and wettability of superhydrophobic silanized inorganic glass coating surfaces textured with a picosecond laser. *Applied Surface Science*, 537(September 2020), 147808. <https://doi.org/10.1016/j.apsusc.2020.147808>

- Ouchene, A., Mollon, G., Ollivier, M., Sedao, X., Pascale-Hamri, A., Dumazer, G., & Serris, E. (2023). Roughness and wettability control of soda-lime silica glass surfaces by femtosecond laser texturing and curing environments. *Applied Surface Science*, 630(March), 157490. <https://doi.org/10.1016/j.apsusc.2023.157490>
- Pan, C., Chen, K., Liu, B., Ren, L., Wang, J., Hu, Q., Liang, L., Zhou, J., & Jiang, L. (2017). Fabrication of micro-texture channel on glass by laser-induced plasma-assisted ablation and chemical corrosion for microfluidic devices. *Journal of Materials Processing Technology*, 240, 314–323. <https://doi.org/10.1016/j.jmatprotec.2016.10.011>
- Parvate, S., Dixit, P., & Chattopadhyay, S. (2020). Superhydrophobic Surfaces: Insights from Theory and Experiment. *Journal of Physical Chemistry B*, 124(8), 1323–1360. <https://doi.org/10.1021/acs.jpcc.9b08567>
- Peethan, A., Aravind, M., & George, S. D. (2023). Surface Wettability and Superhydrophobicity. In *Advances in Superhydrophobic Coatings* (pp. 1–25). Royal Society of Chemistry. <https://doi.org/10.1039/9781837670031-00001>
- Qahtan, T. F., Gondal, M. A., Alade, I. O., & Dastageer, M. A. (2017). Fabrication of Water Jet Resistant and Thermally Stable Superhydrophobic Surfaces by Spray Coating of Candle Soot Dispersion. *Scientific Reports*, 7(1), 1–7. <https://doi.org/10.1038/s41598-017-06753-4>
- Qian, W., Hua, Y., Chen, R., Xu, P., & Yang, J. (2020). Fabrication of superhydrophobic nickel-aluminum bronzes using picosecond laser for enhancing anti-corrosion property. *Materials Letters*, 268, 127570. <https://doi.org/https://doi.org/10.1016/j.matlet.2020.127570>
- Qian, Y., Liu, H., Zhang, L., Jiang, M., Huang, H., & Yan, J. (2023). Tailoring the surface characteristic of metallic glass for wettability control. *Journal of Materials Research and Technology*, 24, 7040–7046. <https://doi.org/10.1016/j.jmrt.2023.05.004>
- Shin, J. (2019). Investigation of the surface morphology in glass scribing with a UV picosecond laser. *Optics and Laser Technology*, 111(September 2018), 307–314. <https://doi.org/10.1016/j.optlastec.2018.10.008>
- Shin, J., & Nam, K. (2020). Groove formation in glass substrate by a UV nanosecond laser. *Applied Sciences (Switzerland)*, 10(3). <https://doi.org/10.3390/app10030987>
- Soldera, M., Alamri, S., Sürmann, P. A., Kunze, T., & Lasagni, A. F. (2021). Microfabrication and surface functionalization of soda lime glass through direct laser interference patterning. *Nanomaterials*, 11(1), 1–17. <https://doi.org/10.3390/nano11010129>
- Stalder, A. F., Kulik, G., Sage, D., Barbieri, L., & Hoffmann, P. (2006). A snake-based approach to accurate determination of both contact points and contact angles. *Colloids and Surfaces A: Physicochemical and Engineering Aspects*, 286(1–3), 92–103. <https://doi.org/10.1016/j.colsurfa.2006.03.008>
- Sui, L., Chen, C., & Zhang, M. (2022). Different Oxidation Methods on the Wetting and Diffusion Characteristics of 304 Stainless Steel on High Alumina Glass. <https://doi.org/https://doi.org/10.21203/rs.3.rs-2168738/v1>
- Vieira, T. M., Sagás, J. C., Pessoa, R. S., & Fontana, L. C. (2020). Multiphase titanium suboxides films grown on glass substrate: Surface energy, wettability and morphology analysis. *Surfaces and Interfaces*, 20(July), 100610. <https://doi.org/10.1016/j.surfin.2020.100610>
- Wang, B., Hua, Y., Ye, Y., Chen, R., & Li, Z. (2017). Transparent superhydrophobic solar glass prepared by fabricating groove-shaped arrays on the surface. *Applied Surface Science*, 426, 957–964. <https://doi.org/10.1016/j.apsusc.2017.07.169>

- Wang, Q., Liu, C., Yin, K., Zhou, Y., & Wang, H. (2023). High-throughput laser-based surface functionalization for fabrication of superhydrophobic soda-lime glass. *International Journal of Applied Glass Science*. <https://doi.org/10.1111/ijag.16643>
- Wang, Z., Ren, Y., Wu, F., Qu, G., Chen, X., Yang, Y., Wang, J., & Lu, P. (2023). Advances in the research of carbon-, silicon-, and polymer-based superhydrophobic nanomaterials: Synthesis and potential application. *Advances in Colloid and Interface Science*, 318(May), 102932. <https://doi.org/10.1016/j.cis.2023.102932>
- Yamaguchi, M., & Kato, S. (2023). Direct-micro-fabrication of Hydrophobic Surface with Re-entrant Texture on Metal Produced by Femtosecond-pulsed Laser. *Lasers in Manufacturing and Materials Processing*, 10(1), 64–76. <https://doi.org/10.1007/s40516-022-00198-y>
- Yang, L., Luo, X., Chang, W., Tian, Y., Wang, Z., Gao, J., Cai, Y., Qin, Y., & Duxbury, M. (2020). Manufacturing of anti-fogging super-hydrophilic microstructures on glass by nanosecond laser. *Journal of Manufacturing Processes*, 59(July), 557–565. <https://doi.org/10.1016/j.jmapro.2020.10.011>
- Yusuf, Y., Ghazali, J., Fadzli, M., Abdollah, B., Teknologi, F., Mekanikal, K., & Pembuatan, D. (2022). Self-cleaning plasma sprayed TiO₂ coatings modified by laser surface texturing process. *Jurnal Tribologi*, 34(November 2021), 39–55.
- Zhang, J., Chen, F., Lu, Y., Zhang, Z., Liu, J., Chen, Y., Liu, X., Yang, X., Carmalt, C. J., & Parkin, I. P. (2020). Superhydrophilic–superhydrophobic patterned surfaces on glass substrate for water harvesting. *Journal of Materials Science*, 55(2), 498–508. <https://doi.org/10.1007/s10853-019-04046-x>
- Zhang, Z. H., Wang, H. J., Liang, Y. H., Li, X. J., Ren, L. Q., Cui, Z. Q., & Luo, C. (2018). One-step fabrication of robust superhydrophobic and superoleophilic surfaces with self-cleaning and oil/water separation function. *Scientific Reports*, 8(1), 1–12. <https://doi.org/10.1038/s41598-018-22241-9>
- Zhao, D., Zhu, H., Zhang, Z., Xu, K., Lei, W., Gao, J., & Liu, Y. (2022). Transparent superhydrophobic glass prepared by laser-induced plasma-assisted ablation on the surface. *Journal of Materials Science*. <https://doi.org/10.1007/s10853-022-07507-y>
- Zhong, W., Wu, M., Xiong, B., Liu, Q., & Liao, H. (2022). High stability superhydrophobic glass-ceramic surface with micro–nano hierarchical structure. *Ceramics International*, 48(16), 23527–23535. <https://doi.org/10.1016/j.ceramint.2022.04.350>
- Zhou, S., Hu, Y., Huang, Y., Xu, H., Wu, D., Wu, D., & Gao, X. (2024). Preparation of Polytetrafluoroethylene Superhydrophobic Materials by Femtosecond Laser Processing Technology. *Polymers*, 16(1). <https://doi.org/10.3390/polym16010043>